

Bio-inspired Robot Design Considering Load-bearing and Kinematic Ontogeny of Chelonioidea Sea Turtles

Andrew Jansen¹, Kevin Sebastian Luck², Joseph Campbell², Heni Ben Amor²,
and Daniel M. Aukes³

¹School of Life Sciences,

²The School of Computing, Informatics, and Decision Systems Engineering,

³The Polytechnic School,

Arizona State University

{majanse1, ksluck, jacampb1, hbenamor, danaukes}@asu.edu

Abstract. This work explores the physical implications of variation in fin shape and orientation that correspond to ontogenetic changes observed in sea turtles. Through the development of a bio-inspired robotic platform – CTurtle – we show that 1) these ontogenetic changes apparently occupy stable extrema for either load-bearing or high-velocity movement, and 2) mimicry of these variations in a robotic system confer greater load-bearing capacity and energy efficiency, at the expense of velocity (or vice-versa). A possible means of adapting to load conditions is also proposed. We endeavor to provide these results as part of a theoretical framework integrating biological inquiry and inspiration within an iterative design cycle based on laminate robotics.

Keywords: Bio-inspired Robots, Turtles, Locomotion, Mobile Robots, Kinematics, Rapid-prototyping, Laminates, Granular Media, Fabrication, Design

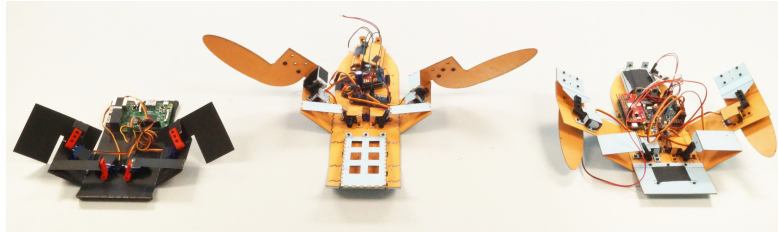


Fig. 1: Three generations of a sea turtle-inspired robot.

1 Introduction

The use of robotics to answer questions in biology is a well-established paradigm which offers benefits to both fields. For biologists, the ability to study repeatable physical systems is an attractive option, even if such systems replicate only a small part of the biological analog. Robotic platforms can be modified quickly to test a wide range of morphologies and behaviors, and sensors can be mounted both in-situ and in the surrounding environment to determine the effect of morphological and behavioral changes on the body and to the world. Such platforms

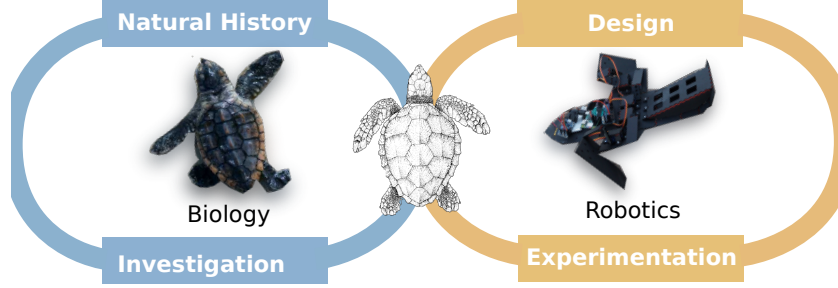


Fig. 2: Our workflow and design cycle for biomimicry. We begin by examining the natural history of the study organisms (Cheloidioidea), from which we draw inspiration for an initial design iteration. This design is simplified and customized using an iterative approach to optimize functionality. During this process, we iterate over numerous parameters of the design, leading to further questions about emergent behaviors and physical principles in both the robotic and the biological systems. Further investigation of the biological system then leads to additional biological observation and mimicry in design variables not considered in the previous design cycle.

have made it possible to understand more about the locomotion of caterpillars, geckos, and sea-turtles, to name a small selection [1–3]. A thorough review is provided by Ijspeert [4].

For roboticists, such collaborations offer insights into robotic design strategies that takes into account knowledge of how species' adaptations make them suited for certain activities or environments. Many have found that such insights successfully transfer to robotic designs inspired by, for example, cockroaches [5–9], geckos [10], bees [11], and sea turtles[12]. Such insights lead both to improved robotic designs and to a better understanding of biological systems.

These studies are often made possible through technological and manufacturing innovations which facilitate the rapid design and fabrication of robotic systems. Many of the platforms cited above make use of rapid prototyping techniques such as 3D printing [1], multi-material laminate fabrication processes [8, 9, 11], or iterative processes such as Shape Deposition Manufacturing(SDM) [6, 10]. Such methods enable the manufacturing of monolithic systems where sub-components exhibit vastly different material properties and performance due to the targeted placement of rigid and soft materials.

We propose a workflow for bio-inspired robotics in Fig. 2, where design inspiration is drawn from biological systems, then the resulting prototype is used as a physical, manipulable analogue to further investigate the properties of that system. Using this theoretical framework, we present our work exploring the ontogenetic differences in sea turtle morphology and locomotion using a crawling robot as a bio-analogue. We outline in detail (1) the implications of the natural history of sea turtles for our design, and (2) the implications of the observed experimental performance of the robot for sea turtle biology. This process is made possible through the design and fabrication of a robotic analog, CTurtle, which permits us to explore the connection between morphology, load-carrying capacity, and performance on a simplified system which can be thoroughly and repetitively tested (Fig. 1).

2 Background: Movement of Turtles

The selection of sea turtles is motivated by three aspects of their locomotion that we identified as promising for this particular application. First, sea turtles are capable of effective movement through unstable media, without loss of traction or sinking; the broad surface area, upturned plastron, and “crutching” motion of the body and fins avert sinking or digging into the substrate, preventing the animal from getting stuck under normal conditions [13, 14]. Secondly, the low center of mass of the turtle and intermittent contact with the ground make the body inherently stable and difficult to overturn; as such, only two limbs are needed to generate forward thrust, making this form of locomotion simple to mimic, easy to manipulate, and amenable to our laminate manufacturing approach. Finally, the unique kinematic behavior of sea turtles can either enable rapid movement of the hatchlings or permit the large and exceedingly heavy adults [up to 915 kg in *Dermochelys coriacea* (Vandelli, 1761)] to move more slowly through granular media, but under considerable load [15, 16].

While there are many differences between species, sea turtle locomotion does exhibit some common variation as a function of development, especially when comparing the hatchling and adult phases of life [13, 14, 17–19]. During the hatchling phase, the young, comparatively lightweight turtles favor speed over load-bearing capacity to escape predation [13, 14, 17, 19]. In particular, hatchling locomotion is characterized by use of the palmar and plantar surfaces of the limbs to compact loose media and generate forward motion, with the arms relatively straight [13, 14, 17, 19]. Compared to adults, hatchlings have more flexible fins to induce substrate compaction while minimizing limb slippage [3, 17]. Furthermore, the body shape of hatchling sea turtles is comparatively narrow, with relatively long limbs; their morphology and gait permits some species to elevate the body fully above ground during motion [17–19].

By contrast, the older, heavier adult turtles move more slowly, especially in heavier species [13, 14, 19]. Adult Chelonioid locomotion is generally characterized by the use of the humerus and radial edge of fin to elevate and advance the body, as if moving on crutches [13, 14, 19]. This occurs with alternating ventral extension and flexion of the humerus, while the radius remains at an approximate 80-90° angle to the humerus, thus crawling on the elbows [13, 14, 19]. Paired movement of both forelimbs in this “crutching” motion elevates center of mass to reduce friction [13, 14]. Compared to hatchlings, the fins of adult sea turtles are much stiffer, more muscular, and comparatively shorter for swimming [13, 14, 19]. This fin morphology, combined with the relatively broad body and paired forelimb motion, greatly reduces the speed of terrestrial locomotion in adults, but enables them to carry a much heavier load [13–16, 19]. Juveniles, although rarely observed on land, have been documented using either of these gaits (with no known intermediate state), and adults appear to learn new gaits in response to morphological differentiation during the maturation process [13, 19, 20].

We believe that the observed decrease in relative speed and increased load-bearing capacity of adult sea turtle locomotion are the result of using a shorter lever arm (palm is distal to humerus) to elevate and advance the body. In this case, the shorter moment arm provides more direct support of center of mass due to the position of humerus; conversely, the longer moment arm of the hatchling fins provides greater apical velocity. From these observations, we predict that a sand crawling robot can be modified to maximize its load-bearing capacity

or velocity by changing the design of its fins to mimic these particular aspects of sea turtle ontogeny. Hatchlings are known for their high energetic needs for rapid escape to the ocean during “hatchling frenzy” [19]. However, it is unknown whether the energy efficiency of these competing forms of locomotion are influenced by their kinematic properties or are determined solely by age, size, and muscle development. The issue of optimizing motion under load for travel distance and energy consumption is critical in battery operated robots.

Based on the reasoning and biological observations presented above, we evaluate the following hypotheses: **1)** In keeping with the results of Mazouchova et al. [3], we hypothesized that limb flexibility aids in substrate compaction and enhances forward motion. **2)** We hypothesize that rotation of the limb about the humeral angle with age, as seen in adult locomotion, reduces the moment arm of the forelimb, increasing load bearing capacity at the expense of velocity. **3)** Given the shorter moment arm of the forelimbs, we hypothesize that adult style locomotion will be more energy efficient than that of hatchlings.

3 Design and Fabrication of the Robotic Sea Turtle

To test our hypotheses, we mimic the change in fin orientation and usage seen during sea turtle development using a turtle-inspired robot which uses three detachable fin designs, where an ellipsoid representing the fin is rotated about the lateral angle of the attachment point, as seen in Fig. 3b, with each design roughly corresponding to a specific developmental state. **1)** The first design was an unrotated (longitudinal) ellipsoidal fin that mimics the hatchling fin morphology. **2)** The second fin design is identical in shape to the first, but is rotated laterally by 90° (transverse). This rotation created an L-shaped base that is similar to the humeral angle of adult sea turtle fins. **3)** The third design was a fin rotated laterally by 45° (diagonal). This configuration does not correspond to any known position adopted by a sea turtle, but rather, simulates an intermediate configuration between the two previous states.

For each fin design, we developed a kinematic model to examine what differences in motion and fin shape might have affected their experimental trajectories. In the experiments, we applied successively heavier loads to the crawler to assess fin performance with a hand-coded controller (see section 3.1). In particular, we measured the total distance traveled with two repetitions of fin motion while (1) varying the angle of the fin in relation to the body, (2) changing the composition and stiffness of the fins, and (3) imposing a load either on the front or back end of the robot. We additionally measured power consumption for the adult and hatchling inspired fins, to address our third hypothesis. Based on the results of this work, we consider the implications of our data as a physical analogue for understanding the ontogeny of terrestrial locomotion in Chelonioidea, and briefly explore possible design changes to allow our robot to dynamically respond to imposed loads via alteration of fin angle.

3.1 Kinematic Modeling

Explicit kinematic models were generated based on the paired four-bar mechanisms (see Fig. 3a) used to elevate the arm of CTurtle and actuate the fin, which are reasonably accurate compared to the actual motion recorded in Figs. 4a and 4b. These models (Fig. 5a and Fig. 5b) show a shortened fulcrum based on fin

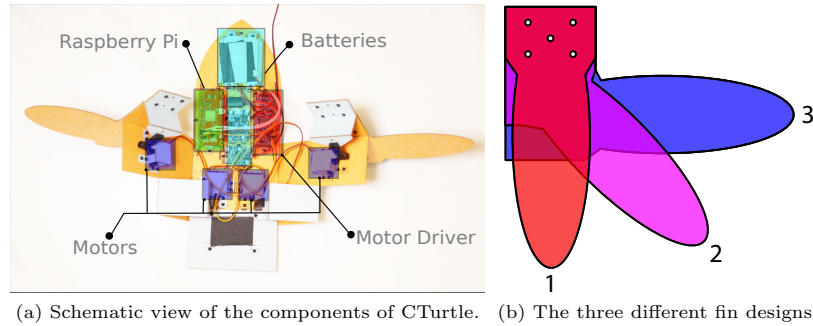


Fig. 3: The final robotic design CTurtle inspired by sea turtles. Figure (b) highlights the three different fin designs tested on the robot: (1) longitudinal fin, (2) intermediate fin and (3) transverse fin.

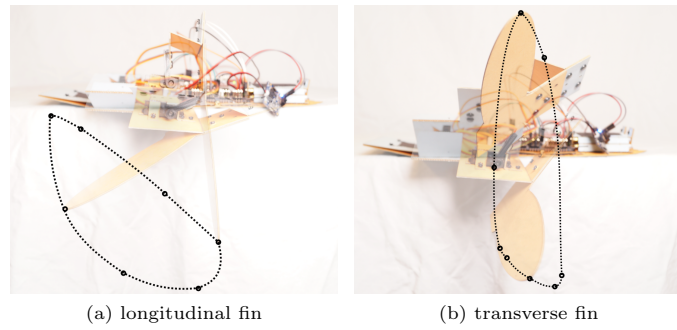


Fig. 4: Lateral views of apical fin motion for (a) the hatchling inspired longitudinal fin, and (b) the adult inspired transverse fin.

rotation about the lateral attachment point, especially for the transverse fin. Figure 5b clearly shows in the lateral (see also Figs. 4a and 4b) and anterior views that the humeral angle of the transverse fin penetrates the substrate (ground at $z = 0$) at approximately 2/3 of the depth attained by longitudinal fin, and with only 1/2 of the maximum forward stroke length.

The open-loop controllers used to generate the motor commands were hand-designed sinusoidal functions offset by 180° to allow sweeping of the fin during the downstroke of the arm, followed by resetting of the fin during the arm upstroke. The sweeping angles of the fin and total identical number of commands given to each motor for each fin design were identical; the time per command and total time per cycle were also identical for each motor and between fin designs (i.e. radial velocity). Thus, rather than try to calculate velocity, we refer to distance travelled per cycle, because each cycle uses the same number of angle commands and uses the same amount of time. In addition, because all fin designs use exactly the same span of angles during the compression of substrate, we are able to effectively eliminate the effect of varying gear ratio as a possible confounding effect on force transmitted to substrate. The importance of this consistency can be seen in Fig. 5c, which shows that transmission efficiency

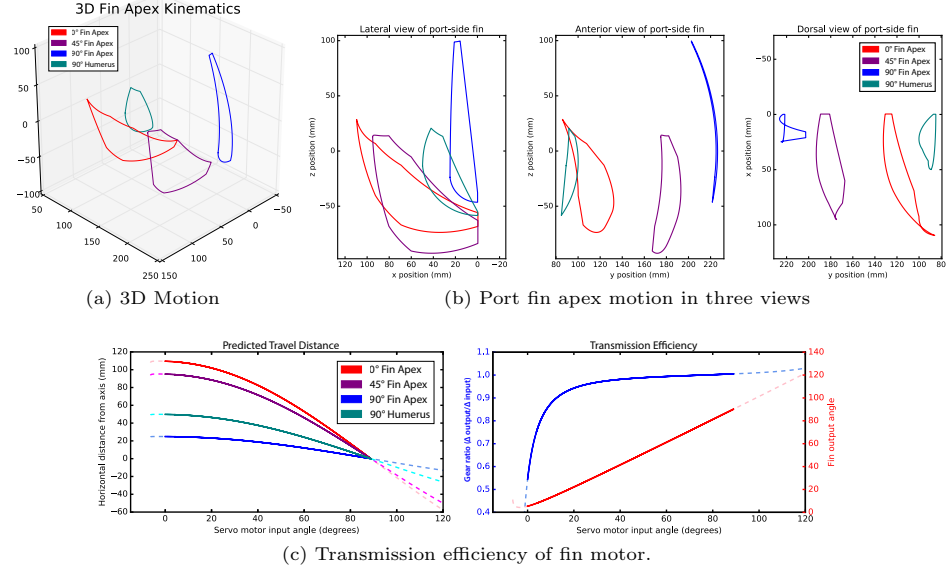


Fig. 5: (a) Three-dimensional motion of port fin apex, viewed laterally from robot mid-line. (b) Motion of port fin apex (and humeral angle of transverse fin) throughout entire stroke; viewed from lateral, anterior, and dorsal views, respectively. (c) Output angle of port fin with respect to arm-mounted servo (fin motor), as well as gear ratio of 4-bar mechanism to which these angles belong; upper panel indicates predicted x-axis coordinate of the fin apex. Dashed lines indicate full range of motion of servo motor, while thicker line represents joint angles used in experiments. In all figures, robot arm is centered at origin, with the fin downstroke generated by 0-90° motor angles.

(with respect to gear ratio) increases with motor angle, providing more effective compression of substrate as the stroke progresses.

The only difference was the magnitude of the downstroke, which was adjusted for each fin design to maximize ground penetration and distance travelled, while minimizing backplowing of the substrate on upstroke. Consequently, in the longitudinal fin, compression of the substrate occurred near the fin apex, similar to hatchling sea turtles [13, 17]. In the transverse fin, substrate compression happened more evenly along the radial edge of the fin and especially near the extended basal portion (analogous to the humeral angle), similar to adult sea turtles [13, 14, 19].

These kinematics imply that, compared to the longitudinal fin, the transverse fin has shorter (Fig. 5c), shallower strokes, with comparatively low apical velocity (due to shorter effective radius of the fin). However, due to the shorter moment arm that creates this pattern, transverse fin was predicted to provide greater force per stroke, and reduced lifting of the body, given the posterior arrangement of components (Fig. 3a). Given the reduced lifting, we predicted greater energy efficiency for transverse fin, due to reduced energy wasted on upward motion.

4 Experiments

Two different experiments were conducted to investigate the hypotheses made in Sec. 2. The first experiment is designed to evaluate hypothesis 1 by measur-

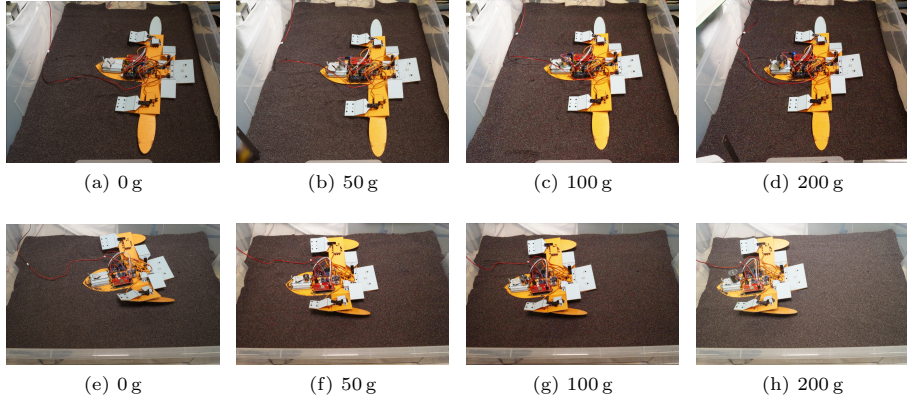


Fig. 6: Final position after the execution of two complete gait cycles with different additional weights carried by the robotic device. In the upper row (a-d) the transverse fin design is used and in the lower row (e-h) the longitudinal fin design is used.

ing the locomotion performance of CTurtle with fins of different stiffness. The second experiment addresses hypotheses 2 and 3 by measuring locomotion performance and energy efficiency of fins with varying rotational angle inspired by their biological counterparts.

4.1 Experimental Setup

All experiments were conducted with the CTurtle robotic platform shown in Fig. 3a. In order to guarantee reproducibility of results, the robot was powered with an external 5 V, 2 A power source as opposed to the onboard batteries in the schematic. Experiments were performed in a simulated sand environment consisting of poppy seeds, in order to avoid the detrimental effect that actual sand has on equipment. The similar granularity between poppy seeds and sand makes it a suitable replacement, despite the difference in density – 0.54 $\frac{g}{ml}$ to 1.46 $\frac{g}{ml}$, respectively. Unlike previous work [12], the motor commands for a gait cycle were derived from a hand-coded combination of sinusoidal functions with a shift of 180° between the functions for vertical and horizontal movements. Joint angles relative to the middle position are given by

$$\begin{aligned} a_{1,4} &= \cos(180^\circ + \frac{t}{T} \cdot 360^\circ \cdot 2) \cdot 60, \\ a_{2,3} &= \sin(180^\circ + \frac{t}{T} \cdot 360^\circ \cdot 2) \cdot m + o \end{aligned} \quad (1)$$

with $a_{1,4}$ being the joint angles for horizontal movements and $a_{2,3}$ for vertical movements. For each of the three different fin designs the vertical movements were adapted to achieve an optimal movement for each fin design with no additional load. For both longitudinal and intermediate fins, the magnitude m was 20 while the transverse required a magnitude of 60 to lift the fin high enough. The offset o for the longitudinal, intermediate and transverse were 10, -15 and -40, respectively.

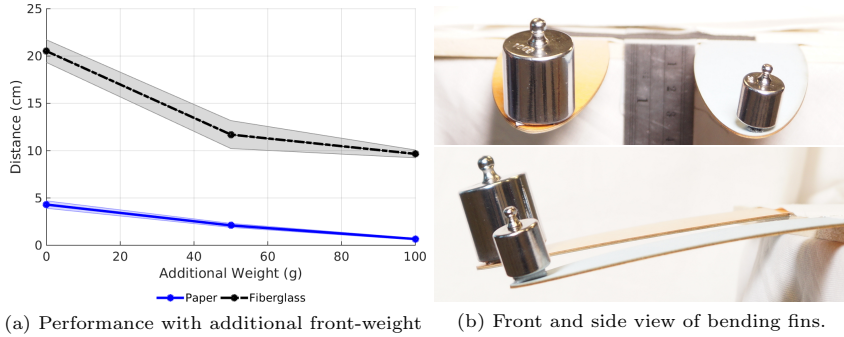


Fig. 7: (a) Evaluation of the performance of rigid fins (fiberglass-reinforced laminate) and flexible fins (paper laminate). The graph shows the mean and standard deviation of five executions for each data point. (b,c) Fiberglass-reinforced (orange) and paper (blue) fins with the same bending radius for 100 g (orange) and 20 g (blue) of weight.

4.2 Measuring the Effect of Fiberglass Reinforcement

For this experiment, we created two sets of fins that vary in rigidity. Flexible, pliant fins were created with a 3-layer laminate consisting of two 6-ply paper layers held together by a 1-ply adhesive layer. Rigid fins were created by reinforcing the 3-layer laminate design with two additional layers of a fiberglass coating (as well as two additional adhesive layers) resulting in a 7-layer laminate. Each set consists of a longitudinal fin and a transverse fin (Fig. 3b) in order to determine whether rigidity performance is affected by the rotational angle of the fin.

The fins were evaluated by attaching them to CTurtle and measuring how far it traveled in the simulated sand environment after executing two complete gait cycles. Each evaluation was performed five times to capture the mean and standard deviation. This process was repeated for load weights varying from 0 g to 100 g, with the weight placed near the front of the robot.

4.3 Evaluating Performance of Different Fin Angles

For the second experiment, we again measured the travel distance of CTurtle in a simulated sand environment, but for all fin designs (Fig. 3b) and for a larger range of load weights. Furthermore, this experiment explored the effect of center of mass on locomotion performance. Evaluations were performed with weights varying from 0 g to 300 g placed at the rear of the robot – in effect moving the center of mass to the rear of CTurtle – and again with weights varying from 0 g to 200 g placed at the front of the robot – forcing the center of mass further forward. All evaluations were performed with rigid, fiberglass-reinforced fins for two complete gait cycles and five repetitions.

An additional set of evaluations was performed to test the energy efficiency of the transverse fin and longitudinal fin designs. The current consumption of all four motors powering CTurtle’s limbs were measured with a DC current sensor operating at 60 Hz while two complete gait cycles were executed. The mean and standard deviation for three repetitions were captured.

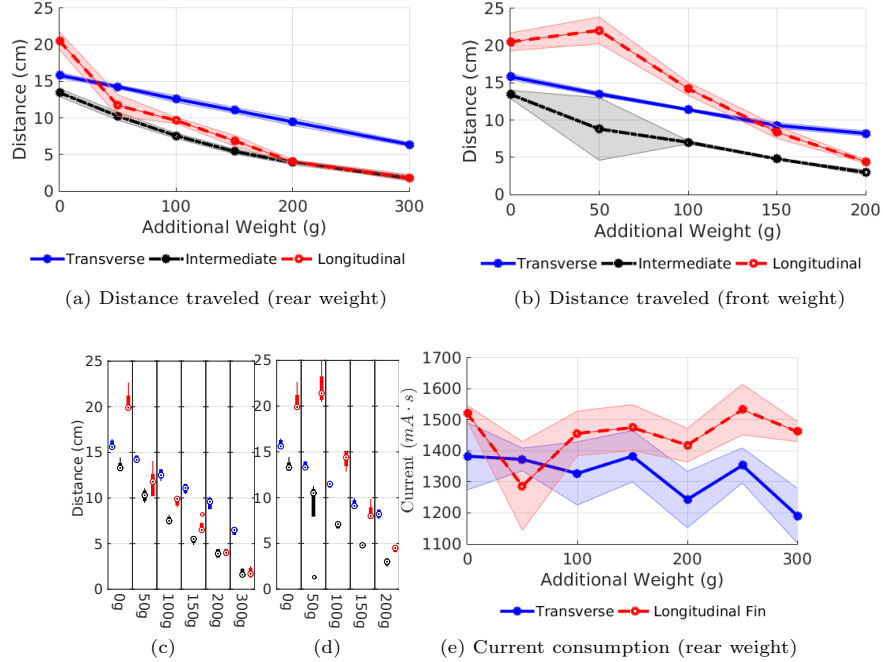


Fig. 8: Performance of CTurtle for the three different fin designs with an additional payload weight of 0-300 g. Figures (a) and (b) show the distance traveled with varying weights placed at the rear and front of CTurtle’s frame, respectively. Each data point represents the mean of five evaluations with the shaded area indicating the standard deviation. Figures (c) and (d) indicate the median, 25%, and 75% quantile for the same evaluations as (a) and (b). Figure (e) shows the mean current consumption of three evaluations for varying weights placed at the rear of CTurtle’s frame.

5 Results

The results of the first experiment, shown in Fig. 7 indicate that the rigid, fiberglass-reinforced fins yield longer travel distance than the flexible, paper fins across all tested loads. The results for the second experiment are shown in Fig. 6 and Fig. 8 and show that the transverse fin configuration enables CTurtle to travel longer distances than the other fin designs with a heavier load. The longitudinal fin design yields the greatest distances for low loads, however, the performance degrades more rapidly than that of the longitudinal fin design with an increasing load, falling behind when the load is 50 g (Fig. 8a) or 150 g (Fig. 8b) depending on the center of mass. The intermediate fin design performs the worst, yielding the shortest traveled distance for all but the highest loads.

Another interesting result is the measured current consumption for the different fin designs, as shown in Fig. 8e. The transverse fin yielded lower current consumption as the additional rear-weight increased, reaching a low of 1191 mA·s for 300g of additional weight. The longitudinal fin, on the other hand, displayed an increasing current consumption trend as the rear-weight increased with 1462 mA·s at the same weight; this is approximately a 22% increase over the transverse fin at the maximum tested load.

6 Discussion

Our results demonstrate that fiberglass reinforcement of the fins indeed leads to improved locomotion, as indicated by a substantial increase in the distance travelled per stroke (Fig. 7). In our robot, fin flexibility is detrimental to locomotor output, which is not fully aligned with the results of Mazouchova et al. [3], where a flexible wrist aided in granule compaction, thus enhancing motion [21, 22]. Most likely this is due to the entire fin being uniformly flexible in our experiment, rather than flexing along a single joint.

Under imposed load, the longitudinal fin travels a greater distance per stroke than the transverse fin. The superiority of the longitudinal fin ends after adding a mere 50 g of additional weight at the back of the robot. Interestingly, the longitudinal fin travelled further with the addition of 50 g to the front end; we believe that the imposed load caused decreased lifting of the front end, leading to earlier fin contact with the ground in each movement cycle. However, even with this increase, the performance of the transverse fin overtakes the longitudinal fin after the addition of 150 g. We surmise that this happens due to differences in the length of the lever arm, which is considerably shorter in the transverse fin (see Fig. 5b). A comparatively long lever arm contributes to per-stroke travel distance at the expense of energy efficiency and load-bearing capacity.

On the design side, these results imply that even a slight increase of battery capacity will require the use of the transverse fin for effective locomotion unless weight redistribution is considered. In general, the results suggest that improved locomotion and energy efficiency is possible with anterior redistribution of battery weight. This, in turn, could be the input into the next iteration of the proposed design pipeline.

In addition to possibly informing future decisions within the next design cycle, these differences in locomotive performance can improve our understanding of sea turtle biology. Hatchling sea turtles have longer limbs in proportion to their body, and, more importantly, compact substrate at a more distal location (palmar surface) on the fore-limbs than adults [13, 14, 17–19]. This gives them a longer moment arm at the shoulder joint (scapula to palmar surface). Based on our results, an elongate moment arm and relatively low weight should enable hatchlings to cover ground at a higher velocity per stroke than adults, *before* considering gait. A comparison of the energy consumption rates of the different fins suggests that this may occur at the expense of increased energy expenditure compared to adults; this observation is supported by high lactic acid production (for rapid energy production) characteristic of hatchling metabolism [19, 20].

Adult sea turtles compact substrate and support their body weight at the anatomical equivalent of the elbow, and have proportionately shorter fins than hatchlings (scapula to humeral angle) [13, 14, 18, 19]. With the transverse fin, our robot was able to move substantially heavier loads across the substrate than with the longitudinal fin, apparently at a considerable cost-savings in energy consumed per movement cycle (approx. 20% at 300 g). Per-cycle energy expenditure appears to decrease with increased load with the transverse fin, but increase with load using the longitudinal fin. Notably, this appears to be an intrinsic advantage due to fin morphology rather than purely a result of gait asymmetry (paired motion of forelimbs) as all sets of fins utilized an asymmetric gait in our experiments. We therefore infer that by propping up the body with both forelimbs and using the humerus to bear weight, adult sea turtles are able to carry a heavier mass (relative to body size) than their immature counterparts.

Surprisingly, a fin rotated at an intermediate angle of 45° was inferior to both of the other fins in distance travelled and load-bearing capacity. The 45° rotation would approximately correspond to an enforced 45° abduction of the humerus; this configuration *is not known* to be used in sea turtle locomotion. However, the inferior locomotive capabilities of this arm position suggests that this might not exist at all because its use would result in poor performance. Although we did not collect energy consumption data for the intermediate fin, we posit that anatomically this position would be disadvantageous and would require the arm to actively support the body using constant tension of the pectoralis major rather than passive support on the rigid humerus. This finding corroborates hypotheses reported in the literature that adult gaits are learned after reaching developmental thresholds of fin differentiation and weight gain [13, 14, 19].

In summary, these biological inferences lead us to believe that we could generate a new design that can reconfigure itself to alternatively maximize velocity or minimize total energy expenditure for a given load. This reconfiguration could be as simple as rotating the fin about a set point upon loading, or by shortening the length of the fin according to the magnitude of the load.

7 Conclusion

This paper explores the relationship between (1) an observed ontological shift in Chelonoid locomotion that we use to inform a robotic design cycle, and (2) experimental results from that design iteration, which lead further inferences into sea turtle biology. We have found strong similarities between the locomotive behavior of our bio-inspired robot and what occurs in nature; namely, a longer moment arm generally exhibits higher per-cycle travel distance and energy consumption, but relatively poor load bearing capacity compared to a shorter effective moment arm. We hypothesize, in turn, that we can design a fin that dynamically reconfigures to optimize its velocity or energy use for an imposed load. This design/exploration process can be fed back into additional biological questions. In future work we could examine the interplay between fin surface area and locomotion under varying loads, both in sea turtles and their robotic analogues, beginning the biological investigation and robotic design cycle anew.

References

- [1] T Umedachi, V Vikas, and B A Trimmer. Softworms : the design and control of non-pneumatic, 3D-printed, deformable robots. *Bioinspiration & Biomimetics*, 11(2):025001, 2016. ISSN 1748-3190.
- [2] K Autumn, a Dittmore, D Santos, M Spenko, and M Cutkosky. Frictional adhesion: A new angle on gecko attachment. *The Journal of experimental biology*, 209(Pt 18):3569–79, 2006. ISSN 0022-0949.
- [3] Nicole Mazouchova, Paul B Umbanhower, and Daniel I Goldman. Flipper-driven terrestrial locomotion of a sea turtle-inspired robot. *Bioinspiration & biomimetics*, 8(2):026007, 2013. ISSN 1748-3190.
- [4] Auke J Ijspeert. Biorobotics: Using robots to emulate and investigate agile locomotion. *Science*, 346(6206):196–203, oct 2014. ISSN 0036-8075.
- [5] R Altendorfer, N Moore, H Komsuoglu, Martin Buehler, H.B. Brown Jr., D. Mc-Mordie, U. Saranli, R. Full, and D. E. Koditschek. RHex: a biologically inspired hexapod runner. *Autonomous Robots*, 11(3):207–213, 2001.

- [6] J. G Cham, S. A Bailey, J. E Clark, R. J Full, and M. R Cutkosky. Fast and Robust: Hexapedal Robots via Shape Deposition Manufacturing. *The International Journal of Robotics Research*, 21(10-11):869–882, oct 2002. ISSN 0278-3649.
- [7] Daniel Kingsley, Roger Quinn, and Roy Ritzmann. A Cockroach Inspired Robot With Artificial Muscles. In *2006 IEEE/RSJ International Conference on Intelligent Robots and Systems*, pages 1837–1842. IEEE, oct 2006. ISBN 1-4244-0258-1.
- [8] A.M. Hoover, Erik Steltz, and R.S. Fearing. RoACH: An autonomous 2.4g crawling hexapod robot. In *2008 IEEE/RSJ International Conference on Intelligent Robots and Systems*, pages 26–33. IEEE, sep 2008. ISBN 978-1-4244-2057-5.
- [9] P. Birkmeyer, K. Peterson, and R. S. Fearing. DASH: A dynamic 16g hexapedal robot. *2009 IEEE/RSJ International Conference on Intelligent Robots and Systems*, pages 2683–2689, oct 2009.
- [10] Matthew Spenko, Salomon Trujillo, Barrett Heyneman, Daniel Santos, M.R. Cutkosky, Sangbae Kim, Matthew Spenko, Salomon Trujillo, Barrett Heyneman, Daniel Santos, Mark R. Cutkosky, and M.R. Cutkosky. Smooth vertical surface climbing with directional adhesion. *IEEE Transactions on Robotics*, 24(1):65–74, feb 2008. ISSN 15523098.
- [11] K. Y. Ma, P. Chirarattananon, S. B. Fuller, and R. J. Wood. Controlled Flight of a Biologically Inspired, Insect-Scale Robot. *Science*, 340(6132):603–607, may 2013. ISSN 0036-8075.
- [12] Kevin Luck, Joseph Campbell, Michael Jansen, Daniel McConnell Aukes, and Heni Ben Amor. From the Lab to the Desert : Fast Prototyping and Learning of Robot Locomotion. *Robotics: Science and Systems Conference (RSS2017)*. (Submitted), 2017.
- [13] Jeanette Wyneken. Sea turtle locomotion: Mechanics, behavior, and energetics. In Peter L Lutz, editor, *The Biology of Sea Turtles*, pages 168–198. CRC Press, 1997.
- [14] Sabine Renous and V Bels. Comparison between aquatic and terrestrial locomotions of the leatherback sea turtle (*dermochelys coriacea*). *Journal of Zoology*, 230(3):357–378, 1993.
- [15] Karen L Eckert and Chris Luginbuhl. Death of a giant. *Marine Turtle Newsletter*, 43:2–3, 1988.
- [16] George R Zug and James F Parham. Age and growth in leatherback turtles, *dermochelys coriacea* (testudines: Dermochelyidae): a skeletochronological analysis. *Chelonian Conservation and Biology*, 2:244–249, 1996.
- [17] Nicole Mazouchova, Nick Gravish, Andrei Savu, and Daniel I Goldman. Utilization of granular solidification during terrestrial locomotion of hatchling sea turtles. *Biology Letters*, 6:398–401, 2010.
- [18] Peter Pritchard and Jeanne Mortimer. Taxonomy, external morphology, and species identification. *Research and management techniques for the conservation of sea turtles*, 4:21, 1999.
- [19] C Kenneth Dodd Jr. Synopsis of the biological data on the loggerhead sea turtle *caretta caretta* (linnaeus 1758). 1988.
- [20] Karl U Smith and Robert S Daniel. Observations of behavioral development in the loggerhead turtle (*caretta caretta*). *Science*, 1946.
- [21] Hesam Askari and Ken Kamrin. Intrusion rheology in grains and other flowable materials. *Nature Materials*, 15(12):1274–1279, 2016.
- [22] Chen Li, Tingnan Zhang, and Daniel I. Goldman. A terradynamics of legged locomotion on granular media. *Science*, 339:1408–1412, 2013.